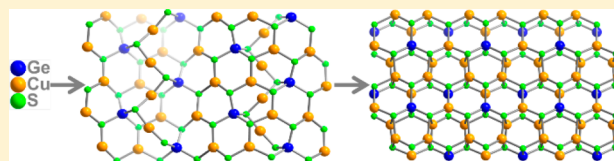


Polymorphic Graphene-like Cuprous Germanosulfides with a High Cu-to-Ge Ratio and Low Band Gap

Qipu Lin,[†] Zhenyu Zhang,[†] Xianhui Bu,[‡] and Pingyun Feng^{*,†}[†]Department of Chemistry, University of California, Riverside, California 92521 United States[‡]Department of Chemistry and Biochemistry, California State University, Long Beach, California 90840 United States

Supporting Information

ABSTRACT: Metal chalcogenides based on heterometallic Ge–Cu–S offer dual attractive features of lattice stabilization by high-valent Ge⁴⁺ and band gap engineering into solar region by low-valent Cu⁺. Herein via cationic amine intercalation, we present three new copper-rich materials with the Cu-to-Ge ratio as high as 3. Two different patterns of Cu–Ge–S distribution could be achieved within each honeycomb sheet. The decoration of such honeycomb sheet by –Cu–S– chain or self-coupling between two honeycomb sheets leads to two layer configurations with different thickness and band gaps. The band gap of these new phases (2.06–2.30 eV), tuned by the layer thickness and the Cu/Ge ratio, represents a significant red shift over known Cu–Ge–S phases with lower Cu/Ge ratios.



INTRODUCTION

Synthesis of advanced materials, from porous materials for fuel storage to semiconducting materials for solar energy conversion, lies at the foundation of emerging technologies.¹ Under structure-directing and charge-density-matching considerations, a new family of metal chalcogenides with various compositions, cluster sizes, and topologies have been developed.² In addition to tetrahedral clusters and their assembly, layered metal chalcogenides with controllable layer composition and thickness are attractive due to the fact that atomic two-dimensional (2D) sheets can allow tailoring of the optoelectronic characteristics of advanced materials.³ For example, the photoelectrochemical performance of MoS₂ can be modulated by controlling the layer thickness.⁴ Compared to graphene, metal chalcogenides are much more diverse in compositions and structures and possess properties that cannot be obtained from graphene whose properties are limited to its unique composition and structure.⁵ Furthermore, layered chalcogenides can also serve as platforms for intercalation chemistry, enabling their applications ranging from adsorbents for removing hazardous radionuclides to solid electrolytes for fast ionic conduction.⁶

In developing chalcogenide materials with novel compositional and topological features, the heterometallic composition has proven fruitful. A number of combinations such as M³⁺/M²⁺ (e.g., In/Zn), M³⁺/M⁺ (e.g., In/Cu) have been studied with the goal of manipulating the size of semiconducting clusters for engineering band structures and framework topologies. In this work, we are interested in a much less studied combination between the high-valent (Ge⁴⁺) and the low-valent (Cu⁺) ions for the following reasons. Because the lattice energy increases with the charge of the metal ion, tetravalent Ge⁴⁺ cations should lead to enhanced stability, compared to, for example, CdS. On the other hand, sulfides

based purely on Ge⁴⁺ tend to have a large band gap, making them less suitable for applications involving solar energy conversion.⁷ As evidenced by earlier studies such as the doping of copper in Cd–In–S nanocluster to enhance photoelectric response,⁸ the incorporation of monovalent Cu⁺ into main group metal sulfides should lead to a significant red shift in the band gap. Moreover, Cu⁺, with various coordination modes, can help generate a variety of structural modes.

The Ge–Cu combination is synthetically more challenging, because the large difference between the charge of metal ions (+4 vs +1) tends to promote the macroscopic phase separation. Still it is possible to achieve nanoscale or even cluster-level separation to yield heterometallic crystalline materials in which different metal ions play complementary roles. So far, only a few extended framework types of Cu–Ge–S are known. Two germanium-rich open frameworks built of T₂-clusters [Ge₄S₁₀]^{4–} linked by Cu⁺ or Cu₂²⁺ bridges have been reported with a Cu/Ge ratio of 0.50 and 1.00, respectively.⁹ Copper-rich framework sulfides containing icosahedral [Cu₈S₁₂]^{16–} clusters bonded to each other via Ge⁴⁺ or [Ge₂S₆]^{4–} units are also known, and they exhibit Cu/Ge ratios of 2.67, 2.0, and 1.6, respectively.^{7,10}

Here we report three heterometallic Cu–Ge–S materials (denoted OCF-91, -92, and -93) based on honeycomb sheets intercalated with cationic amines. One unusual feature is the high concentration of low-valent cuprous sites. To our knowledge, the Cu/Ge ratio of 3 is the highest among open-framework materials. Such a high Cu/Ge ratio has a dramatic effect on its electronic and optical properties, because of the significant orbital contribution from Cu⁺ to the band structure. Another unusual feature is two different Cu/Ge ratios in the

Received: October 7, 2014

Published: November 26, 2014

Table 1. Crystallographic Data and Structure Refinements for Grapheme-like CuGeS Composites

compound reference	OCF-91	OCF-92	OCF-93
chemical formula	Cu ₃ GeS ₄ (H ₂ DAP) _{0.5} ^a	Cu ₃ GeS ₄ (H ₂ DAP) _{0.5} ^a	Cu ₃ GeS ₄ (H ₂ PR) _{0.5} ^a
formula mass	429.56	429.56	435.58
crystal system	orthorhombic	monoclinic	monoclinic
a/Å	6.4955(2)	20.7857(7)	18.6330(4)
b/Å	18.4218(4)	7.4656(2)	7.3801(14)
c/Å	20.1841(4)	13.1562(5)	13.2110(3)
α/deg	90.00	90.00	90.00
β/deg	90.00	116.428(2)	101.299(13)
γ/deg	90.00	90.00	90.00
unit cell volume/Å ³	2415.21(10)	1828.20(10)	1781.5(7)
temperature/K	150(2)	150(2)	150(2)
space group	Pbca	C2/c	C2/c
Z	8	8	8
no. of reflections measured	11 113	6378	8304
no. of independent reflections	2431	1600	1839
R _{int}	0.1024	0.0315	0.0444
final R ₁ ^a values (I > 2σ(I))	0.0320	0.0399	0.0291
final wR(F ²) ^a values (I > 2σ(I))	0.0687	0.1271	0.0792
final R ₁ ^a values (all data)	0.0488	0.0484	0.0366
final wR(F ²) ^a values (all data)	0.0718	0.1338	0.0834
goodness of fit on F ²	0.978	1.036	1.049

^aDAP = 1,3-diaminopropane, PR = piperazine, R₁ = $\sum ||F_o| - |F_c|| / \sum |F_o|$, wR = $\{\sum w[(F_o)^2 - (F_c)^2]^2 / \sum w[(F_o)^2]^2\}^{1/2}$.

graphene-like sheet. OCF-91 has charge-neutral 2Cu:1Ge:3S six-membered rings, while OCF-92 and -93 consist of two types of six-rings: 3Cu:3S and 2Cu:1Ge:3S. Such two different ring configurations create two different mechanisms to satisfy the tetrahedral coordination of Ge sites located within the honeycomb sheet: -Cu-S- chain decoration versus self-coupling to form double-deck. As a result, polymorphic layers with different layer configuration and thickness are obtained.

EXPERIMENTAL SECTION

Materials and General Methods. All reagents and solvents employed in the synthetic study were commercially available and used as supplied without further purification. Solid-state diffuse reflectance spectrum was recorded on a Shimadzu UV-3101PC UV-vis-NIR Scanning Spectrophotometer by using BaSO₄ powder as 100% reflectance reference. Powder X-ray diffraction (XRD) pattern was collected using a Bruker D8-Advance powder diffractometer operating at 40 kV, 40 mA with Cu Kα (λ = 1.540 56 Å) radiation (2θ range, 4–40°; step, 0.02°; scan speed, 2 s/step).

Synthesis of OCF-91. (Cu₃GeS₄·0.5H₂DAP). A mixture of copper powder (Cu, 0.044 g, 0.6 mmol), germanium powder (Ge, 0.050 g, 0.7 mmol), sulfur powder (S, 0.110 g, 3.4 mmol), and 1,3-diaminopropane (DAP, 2.09 g) was prepared and stirred in a 23 mL Teflon-lined stainless steel autoclave for 0.5 h. The vessel was sealed and then heated at 190 °C for 8 d. The autoclave was subsequently cooled to room temperature. Light red crystals were obtained in a yield of ~30% based on Cu.

Synthesis of OCF-92. (Cu₃GeS₄·0.5H₂DAP). A mixture of Cu(OAc)₂·H₂O (0.254 g, 1.3 mmol), GeO₂ powder (0.100 g, 0.9 mmol), sulfur powder (S, 0.348 g, 10.9 mmol), and 1,3-diaminopropane (DAP, 2.06 g) was prepared and stirred in a 23 mL Teflon-lined stainless steel autoclave for 1 h. The vessel was sealed and then heated at 190 °C for 8 d. The autoclave was subsequently cooled to room temperature. Light red block crystals were isolated with a yield of ~34% based on Cu.

Synthesis of OCF-93. (Cu₃GeS₄·0.5H₂PR, where PR = piperazine, produced by the decomposition of 1-(2-aminoethyl)piperazine). A mixture of Cu(OAc)₂·H₂O (1.533 g, 7.6 mmol), GeO₂ powder (0.100 g, 0.9 mmol), sulfur powder (S, 0.367 g, 11.5 mmol), and 1-(2-aminoethyl)piperazine (AEP, 4.16 g) was prepared and stirred in a 23

mL Teflon-lined stainless steel autoclave for 1 h. The vessel was sealed and then heated at 190 °C for 8 d. The autoclave was subsequently cooled to room temperature. Light red block crystals were isolated with a yield of ~35% based on Ge.

Single-Crystal X-ray Diffraction. Single-crystal X-ray analysis was performed on a Bruker SMART APEX II CCD area diffractometer with nitrogen-flow temperature controller using graphite-monochromated Mo Kα radiation (λ = 0.710 73 Å), operating at 50 kV and 30 mA and in the ω and φ scan modes. The SADABS program was used for absorption correction. The structure was solved by direct methods and refined by full-matrix least-squares on F² using SHELXTL software suite.¹¹ Non-hydrogen atoms were refined with anisotropic displacement parameters during the final cycles. Solvent molecules in the lattice of OCF-92 could not be resolved from Fourier maps due to the high degree of positional disorder.

RESULTS AND DISCUSSION

Phase Control with Inorganic Precursors and Organic Structure-Directing Agents. Solvothermal reaction of copper powder, germanium powder, and sulfur powder in a nonaqueous solvent of 1,3-diaminopropane (DAP) led to light red crystals of OCF-91. OCF-92 and OCF-93 were synthesized similarly. Replacement of copper and germanium powders used for OCF-91 with Cu(OAc)₂·H₂O and GeO₂ gave OCF-92 with the same framework formula [Cu₃GeS₄]⁻. On the basis of the OCF-92's reaction condition, OCF-93 was synthesized by substituting DAP with 1-(2-aminoethyl)piperazine (AEP, which decomposed into protonated piperazine to serve as counterion). Crystal structures of all three phases were determined by single-crystal XRD (Table 1). The phase purity was supported by powder XRD. It is also worth noting that the same template can be used to access different structure types, as evidenced by OCF-91 and OCF-92, both of which are directed by DAP cations. The syntheses of OCF-91 and OCF-92 show that the nature of precursor binding of metal ions can be used to alter the self-assembly process of metal chalcogenides.

Enhancing Cu/Ge Ratio through -Cu-S- Chain Decoration of 2Cu-Ge-3S Honeycomb Sheets. OCF-

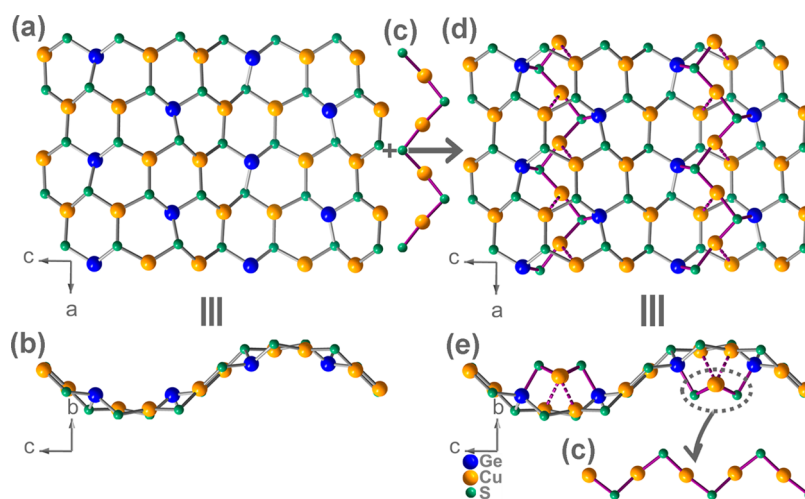


Figure 1. (a, b) Top and side views of 2D undulated honeycomb layer $[\text{Cu}_2\text{GeS}_3]$; (c) side view of a Cu–S chain; (d, e) top and side views of the Cu–S decorated layer in OCF-91 showing zigzag $[\text{CuS}]^-$ chains on both sides of 2D $[\text{Cu}_2\text{GeS}_3]$ layers.

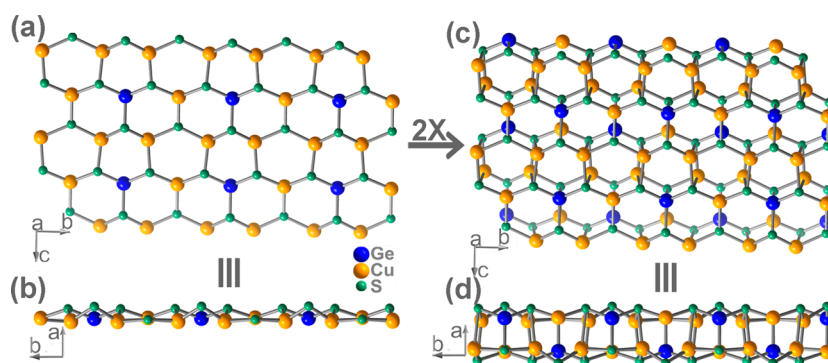


Figure 2. (a, b) Top and side views of 2D honeycomb sheet $[\text{Cu}_3\text{GeS}_4]^-$; (c, d) top and side views of double-layer in OCF-92 and -93.

91 contains a unique 2D anionic sheet, $[\text{Cu}_3\text{GeS}_4]^-$, with protonated DAP molecules in the interlayer void. As depicted in Figure 1, each sheet consists of two parts: –S–Cu–S– zigzag chains and a wavelike layer with a honeycomb-type lattice. The chain is composed of repeating Cu–S units linked by vertex sharing. The undulating graphene-like net is constructed by trigonal CuS_3 units sharing vertices to form a 2D crown-like structure, whose cavities are occupied by Ge^{4+} ions. As a result, each six-ring unit in the graphene-like net is built of two Cu^+ , one Ge^{4+} , and three bridging S^{2-} . Because of the requirement for tetrahedral coordination by Ge^{4+} , a S^{2-} anion must be capped onto one side of each Ge-site, leading to a decorated honeycomb layer formed by interconnection of $[\text{CuS}]^-$ chains and the $[\text{Cu}_2\text{GeS}_3]$ net through the coordination of Ge to S and weak Cu–Cu interactions (with the shortest distance of 2.760 Å).

Self-Coupling of Copper-Rich Honeycomb Sheets. OCF-92 is composed of double atomic layers of $[\text{Cu}_3\text{GeS}_4]^-$ separated by the same organic amine DAP as in OCF-91. In each planar individual layer, there are two kinds of six-ring building units in a 3:1 ratio. The first type is built of two Cu^+ and one Ge^{4+} spaced by three S^{2-} anions, while the second type consists of three Cu^+ ions and three S^{2-} anions. Thus, the composition of each single honeycomb layer in OCF-92 is different from that in OCF-91. Also, to meet the tetrahedral coordination of Ge^{4+} ion, two such individual honeycomb nets are coupled together via Ge–S to give a bilayer arrangement (Figure 2). OCF-93 has the same double-layer structure;

however, layers are separated by charge-balancing protonated piperazine cations instead.

Apart from these layered structures, a three-dimensional (3D) open-framework Cu–Ge–S phase was also isolated under reaction conditions similar to those used for OCF-92 and -93, except that ethylenediamine (en) was used. This 3D open-framework (CuGeS-en) reported earlier⁷ is based on anionic icosahedral $[\text{Cu}_8\text{S}_{12}]^{16-}$ clusters cross-linked by tetrahedral $[\text{GeS}_4]^{4-}$ and dimeric $[\text{Ge}_2\text{S}_6]^{4-}$ units (Figure 3). CuGeS-en has the $\text{Cu}^+/\text{Ge}^{4+}$ molar ratio of 1.6, much lower than that of the layered structures in this work ($\text{Cu}^+/\text{Ge}^{4+} = 3$), highlighting the great effect of structure-directing agents. It is of interest to note that the metal-to-sulfur ratio of all three layered phases synthesized herein is 1, a value that is between 2 and 0.5 for Cu_2S and GeS_2 , respectively.

Red Shift in Optical Band Gaps Tuned by Layer Thickness and Cu/Ge Ratio. Diffuse-reflectance spectra of OCF-91, -92, and -93, together with 3D CuGeS-en, were recorded at room temperature on a Shimadzu UV-3101PC double-beam, double-monochromator spectrophotometer in the wavelength range of 250–800 nm. The purity of the samples was examined by powder XRD prior to the measurement (Figure 4a), and the presence of amine template molecules between layers was supported by Fourier transform infrared (FT-IR) spectroscopy (Figure 4b). As shown in Figure 4c, the optical absorption data derived from the reflectance data show an optical transition with a band gap of 2.30 eV for OCF-91, 2.06 eV for OCF-92, and 2.10 eV for OCF-93. The latter

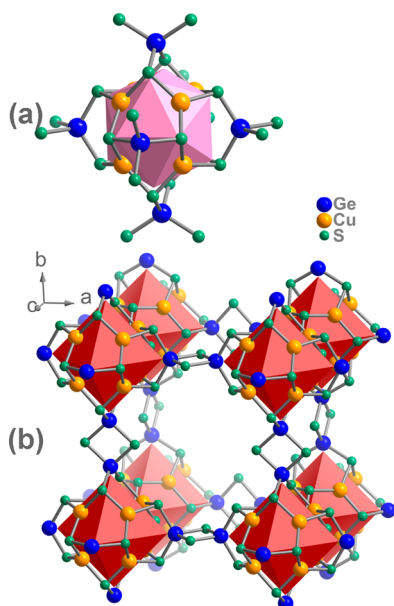


Figure 3. (a) Icosahedral $[\text{Cu}_8\text{S}_{12}]^{16-}$ cluster and its coordination geometry with six Ge^{4+} ions; (b) polyhedral mode of 3D open framework in CuGeS-en (the cations inside are omitted for clarity).

two values are close due to their similar double layers. These band gaps lie in the energy range suitable for visible-light applications. For the layered structures, the band gap of OCF-91 differs significantly from that of OCF-92 (or 93) as a result of the change in the configuration of layers. An increase in the layer thickness in OCF-92 and -93 results in a red shift in the optical absorption. Compared with 3D open-framework phase CuGeS-en (2.47 eV), the band gaps of these layered compounds are significantly red-shifted, which can be mostly ascribed to the contribution of more Cu^+ sites (with higher $\text{Cu}^+/\text{Ge}^{4+}$ molar ratio of 3 in layered phases vs 1.6 in the 3D CuGeS phase) in the lattices.

CONCLUSIONS

In conclusion, a new family of copper-rich Cu–Ge–S hybrid materials with the unprecedented layer configurations have been synthesized, and their crystal structures and optical properties have been characterized. These atomically thick layered materials, bearing $\text{Cu}^+/\text{Ge}^{4+}$ molar ratio as high as 3, exhibit a low electronic band gap. Significantly, it is demonstrated that the Cu/Ge ratio and layer thickness can

be engineered to tune the band structure. The phase sensitivity of the resulting new materials to the chemical nature of metal precursors and structure-directing agents, as demonstrated in this work, reveals the possibility for a rich family of metal chalcogenides in this fascinating heterometallic system.

ASSOCIATED CONTENT

Supporting Information

X-ray crystallographic files, in CIF format (CCDC 1023417 (OCF-91), 1023418 (OCF-92), and 1023419 (OCF-93)). This material is available free of charge via the Internet at <http://pubs.acs.org>.

AUTHOR INFORMATION

Corresponding Author

*E-mail: pingyun.feng@ucr.edu. Phone: +1(951)827-2042. Fax: +1(951)827-4713.

Author Contributions

All authors have given approval to the final version of the manuscript.

Notes

The authors declare no competing financial interest.

ACKNOWLEDGMENTS

We thank the support of this work by the National Science Foundation (Grant No. DMR-1200451 to P.F.).

REFERENCES

- (1) (a) Gonzalez-Leon, J. A.; Acar, M. H.; Ryu, S. W.; Ruzette, A. V.; Mayes, A. M. *Nature* **2003**, *426*, 424–428. (b) Gao, M. R.; Xu, Y. F.; Jiang, J.; Yu, S. H. *Chem. Soc. Rev.* **2013**, *42*, 2986–3017. (c) Jhang, P. C.; Yang, Y. C.; Lai, Y. C.; Liu, W. R.; Wang, S. L. *Angew. Chem., Int. Ed.* **2009**, *48*, 742–745. (d) Lin, H. Y.; Chin, C. Y.; Huang, H. L.; Huang, W. Y.; Sie, M. J.; Huang, L. H.; Lee, Y. H.; Lin, C. H.; Liu, K. H.; Bu, X.; Wang, S. L. *Science* **2013**, *339*, 811–813. (e) Huang, S. H.; Lin, C. H.; Wu, W. C.; Wang, S. L. *Angew. Chem., Int. Ed.* **2009**, *48*, 6124–6127. (f) Liu, T.; Luo, D.; Xu, D.; Zeng, H.; Lin, Z. *Dalton Trans.* **2013**, *42*, 368–371. (g) Xiong, W. W.; Athresh, E. U.; Ng, Y. T.; Ding, J.; Wu, T.; Zhang, Q. *J. Am. Chem. Soc.* **2013**, *135*, 1256–1259. (h) Kang, M. P.; Luo, D. B.; Lin, Z. E.; Thiele, G.; Dehnen, S. *CrystEngComm* **2013**, *15*, 1845–1848. (i) Gao, J.; Cao, S.; Tay, Q.; Liu, Y.; Yu, L.; Ye, K.; Mun, P. C.; Li, Y.; Rakesh, G.; Loo, S. C.; Chen, Z.; Zhao, Y.; Xue, C.; Zhang, Q. *Sci. Rep.* **2013**, *3*, 1853. (j) Hu, B. L.; Wang, C. Y.; Wang, J. X.; Gao, J. K.; Wang, K.; Wu, J. S.; Zhang, G. D.; Cheng, W. Q.; Venkateswarlu, B.; Wang, M. F.; Lee, P. S.; Zhang, Q. C. *Chem. Sci.* **2014**, *5*, 3404–3408. (k) Gao, J.; Miao, J.; Li, P. Z.; Teng, W. Y.; Yang, L.; Zhao, Y.; Liu, B.; Zhang, Q. *Chem. Commun.*

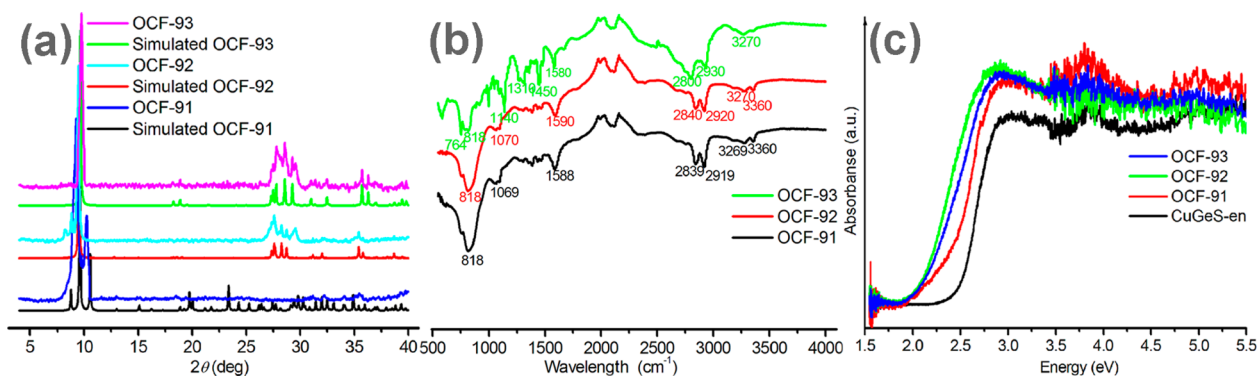


Figure 4. (a) Simulated and measured powder XRD patterns. (b) FT-IR spectra of OCF-91, -92, and -93. (c) The diffuse reflectance spectra of the OCF-91, -92, -93, and CuGeS-en , demonstrating that the red shift could be accomplished by either an increase in Cu/Ge ratio or the layer thickness.

2014, 50, 3786–3788. (l) Zheng, S. T.; Zhang, H.; Yang, G. Y. *Angew. Chem., Int. Ed.* **2008**, 47, 3909–3913. (m) Powell, A. V.; Leyva-Bailen, P.; Vaqueiro, P.; Sanchez, R. D. *Chem. Mater.* **2009**, 21, 4102–4104. (n) Vaqueiro, P.; Romero, M. L.; Rowan, B. C.; Richards, B. S. *Chem.—Eur. J.* **2010**, 16, 4462–4465. (o) Huang, S. H.; Wang, S. L. *Angew. Chem., Int. Ed.* **2011**, 50, 5319–5322. (p) Zheng, S. T.; Zhang, J.; Clemente-Juan, J. M.; Yuan, D. Q.; Yang, G. Y. *Angew. Chem., Int. Ed.* **2009**, 48, 7176–7179. (q) Ewing, S. J.; Vaqueiro, P. *Inorg. Chem.* **2014**, 53, 8845–8847. (r) Vaqueiro, P.; Romero, M. L. *J. Am. Chem. Soc.* **2008**, 130, 9630–9631. (s) Wang, K.; Luo, D.; Xu, D.; Guo, F.; Liu, L.; Lin, Z. *Dalton Trans.* **2014**, 43, 13476–13479. (t) Zhang, X.; Hejazi, M.; Thiagarajan, S. J.; Woerner, W. R.; Banerjee, D.; Emge, T. J.; Xu, W.; Teat, S. J.; Gong, Q.; Safari, A.; Yang, R.; Parise, J. B.; Li, J. *J. Am. Chem. Soc.* **2013**, 135, 17401–17407.

(2) (a) Feng, P. Y.; Bu, X. H.; Zheng, N. F. *Acc. Chem. Res.* **2005**, 38, 293–303. (b) Bu, X.; Zheng, N.; Feng, P. *Chem.—Eur. J.* **2004**, 10, 3356–3362. (c) Han, X.-H.; Wang, Z.-Q.; Liu, D.; Xu, J.; Liu, Y.-X.; Wang, C. *Chem. Commun.* **2014**, 50, 796–798. (d) Wang, K.-Y.; Feng, M.-L.; Li, J.-R.; Huang, X.-Y. *J. Mater. Chem. A* **2013**, 1, 1709–1715. (e) Li, J.-R.; Xiong, W.-W.; Xie, Z.-L.; Du, C.-F.; Zou, G.-D.; Huang, X.-Y. *Chem. Commun.* **2013**, 49, 181–183. (f) Ewing, S. J.; Romero, M. L.; Hutchinson, J.; Powell, A. V.; Vaqueiro, P. *Z. Anor. Allg. Chem.* **2012**, 638, 2526–2531. (g) Lin, Y.; Massa, W.; Dehnen, S. *J. Am. Chem. Soc.* **2012**, 134, 4497–4500. (h) Chen, Z.-Y.; Luo, D.-B.; Luo, X.-C.; Kang, M.-P.; Lin, Z.-E. *Dalton Trans.* **2012**, 41, 3942–3944. (i) Xiong, W.-W.; Li, J.-R.; Hu, B.; Tan, B.; Li, R.-F.; Huang, X.-Y. *Chem. Sci.* **2012**, 3, 1200–1204. (j) Ewing, S. J.; Powell, A. V.; Vaqueiro, P. *J. Solid State Chem.* **2011**, 184, 1800–1804. (k) Lin, Y.; Dehnen, S. *Inorg. Chem.* **2011**, 50, 7913–7915. (l) Zhang, Q. C.; Armatas, G.; Kanatzidis, M. G. *Inorg. Chem.* **2009**, 48, 8665–8667. (m) Zhang, Q. C.; Malliakas, C. D.; Kanatzidis, M. G. *Inorg. Chem.* **2009**, 48, 10910–10912.

(3) (a) Huang, X. Y.; Li, J. *J. Am. Chem. Soc.* **2007**, 129, 3157–3162. (b) Ki, W.; Li, J. *J. Am. Chem. Soc.* **2008**, 130, 8114–8115. (c) Li, J.; Bi, W. H.; Ki, W.; Huang, X. Y.; Reddy, S. *J. Am. Chem. Soc.* **2007**, 129, 14140–14141. (d) Zhang, Q. C.; Bu, X. H.; Han, L.; Feng, P. Y. *Inorg. Chem.* **2006**, 45, 6684–6687.

(4) (a) Lopez-Sanchez, O.; Lembke, D.; Kayci, M.; Radenovic, A.; Kis, A. *Nat. Nanotechnol.* **2013**, 8, 497–501. (b) Ganatra, R.; Zhang, Q. *ACS Nano* **2014**, 8, 4074–4099.

(5) (a) Jeong, S.; Yoo, D.; Jang, J. T.; Kim, M.; Cheon, J. *J. Am. Chem. Soc.* **2012**, 134, 18233–18236. (b) Sun, Y.; Sun, Z.; Gao, S.; Cheng, H.; Liu, Q.; Lei, F.; Wei, S.; Xie, Y. *Adv. Energy Mater.* **2014**, 4, 1300611.

(6) Sengupta, P.; Dudwadkar, N. L.; Vishwanadh, B.; Pulhani, V.; Rao, R.; Tripathi, S. C.; Dey, G. K. *J. Hazard. Mater.* **2014**, 266, 94–101.

(7) Zhang, Z. Y.; Zhang, J.; Wu, T.; Bu, X. H.; Feng, P. Y. *J. Am. Chem. Soc.* **2008**, 130, 15238–15239.

(8) Wu, T.; Zhang, Q.; Hou, Y.; Wang, L.; Mao, C.; Zheng, S. T.; Bu, X.; Feng, P. *J. Am. Chem. Soc.* **2013**, 135, 10250–10253.

(9) (a) Tan, K. M.; Ko, Y. H.; Parise, J. B.; Darovsky, A. *Chem. Mater.* **1996**, 8, 448–453. (b) Bowes, C. L.; Huynh, W. U.; Kirkby, S. J.; Malek, A.; Ozin, G. A.; Petrov, S.; Twardowski, M.; Young, D.; Bedard, R. L.; Broach, R. *Chem. Mater.* **1996**, 8, 2147–2152. (c) Tan, K. M.; Darovsky, A.; Parise, J. B. *J. Am. Chem. Soc.* **1995**, 117, 7039–7040.

(10) (a) Zhang, R.-C.; Zhang, C.; Ji, S.-H.; Ji, M.; An, Y.-L. *J. Solid State Chem.* **2012**, 186, 94–98. (b) Zhang, R. C.; Yao, H. G.; Ji, S. H.; Liu, M. C.; Ji, M.; An, Y. L. *Inorg. Chem.* **2010**, 49, 6372–6374.

(11) (a) Sheldrick, G. M. *SHELXS-97*, PC version; University of Göttingen, Germany, 1997. (b) Sheldrick, G. M. *SHELXTL*, version 5.1; Bruker Analytical X-ray Instruments, Inc.: Madison, WI, 1998. (c) Sheldrick, G. M. *Acta Crystallogr.* **2008**, A64, 112–122.